International Journal of Industrial Chemistry (2019) 10:159–173
https://doi.org/10.1007/s40090-019-0181-8

RESEARCH

Synthesis and investigations of heterocyclic compounds as corrosion inhibitors for mild steel in hydrochloric acid

Salima K. Ahmed[1] · Wassan B. Ali[1] · Anees A. Khadom[2]

Received: 30 July 2018 / Accepted: 14 March 2019 / Published online: 20 March 2019

Abstract
The corrosion inhibition of mild steel in 0.5 M hydrochloric acid by six synthesized heterocyclic compounds was studied using weight loss measurements. The inhibition efficiency exceeded 95%. The excellent inhibitor performance was attributed to the formation of protection adsorption films on the steel surface. The structures of compounds were confirmed by Fourier transform infrared and nuclear magnetic resonance analysis. The adsorption of inhibitor on steel surface followed the Langmuir adsorption isotherm. Quantum chemical calculations were also adopted to clarify the inhibition mechanism.

Keywords Steel · Weight loss · FT-IR · Corrosion · Inhibition · Synthesis

Introduction

Iron and its alloys are widely used as a constructional material in several industrial applications, such as petroleum, power plants, chemical industries due to its high mechanical strength, easy fabrication and low cost [1, 2]. The variety of applications make steel in contact with various corrosive environments, such as acidic solutions during the processes of etching, acid pickling, acid descaling, acid cleaning, oil well acidification. [3]. In acidic media, steel alloys react easily and converted from metallic to ionic state forming a huge economic loss. Therefore, there is a necessary need to develop some excellent corrosion controlling methods. One of the methods is the use of corrosion inhibitors [4–6]. Corrosion inhibitors can be classified according to chemical structure, method of action, etc. One of the common classes is organic corrosion inhibitors that obtained the highest importance due to their ease synthesis at relatively low cost and high protection ability. The method of prevention can be ascribed to the adsorption on the steel surface and impeding the active corrosion sites. Formation of protective layer between the aggressive solution and metal surface hinder the dissolution of the metal and reduce corrosion damages [7, 8]. Organic inhibitors containing heteroatoms, such as N, O, S and P, have proven practically and theoretically to act as efficiently corrosion inhibitors in a wide range of acidic solutions [9, 10]. The efficiency of these inhibitors can be attributed to their high polarizability and lower electronegativity; so that these atoms and the functional groups can cover large metallic surface areas and easily electrons transfer to the empty orbitals of atoms [11]. In addition, nitrogen-containing organic inhibitors is good anticorrosion materials for metals in hydrochloric acid, while compounds having sulfur atoms act as good inhibitors in sulfuric acid. Compounds holding nitrogen and sulfur behave as perfect corrosion inhibitors for both media [12]. The action of any inhibitor for any specific metallic alloys in sever acidic environments depends on the nature of the characteristic inhibitor film accumulated on the metal surface and the number and nature of adsorption centers contributing in the adsorption process. In general, the inhibition performance of the inhibitors having different heteroatoms follows the reverse order of their electronegativities, so that in S, N, O and P, the inhibition performance followed in the order of: O < N < S < P [13]. The existence of organic materials in the acidic solutions commonly alters the electrochemical behavior of the acidic environments. In other words, it decreases the aggressiveness of the solution. The most regularly used heterocyclic compounds have sulfur (S), phosphorus (P), nitrogen (N) or oxygen (O) heteroatoms, and these effectively take part in

✉ Anees A. Khadom
aneesdr@gmail.com

[1] Department of Chemistry, College of Science, University of Diyala, Baquba City 32001, Diyala Governorate, Iraq

[2] Department of Chemical Engineering, College of Engineering, University of Diyala, Baquba City 32001, Diyala Governorate, Iraq

adsorption centers. Therefore, in this study, six heterocyclic compounds were syntheses and selected to act as corrosion inhibitors for steel in hydrochloric acid solution.

Experimental work

Materials and test conditions

All the reagents and starting materials as well as solvents were purchased commercially and used without any further purification. Test sample was carbon steel which has the following chemical compositions (%wt): 0.1 C, 0.335 Mn, 0.033 Si, 0.0067 S, 0.0056 P, 0.057 Al, 0.0476 Cu, 0.0201 Cr, 0.001 Co, 0.0007 Ti and the balance is F. Prior to each measurement, the steel electrode was abraded with emery papers with grade of 800–1500, washed ultrasonically with distilled water, acetone and alcohol, and dried under dry air. Testing electrolyte of 0.5 M HCl aqueous solution was prepared by diluting Analar Grade 37% hydrochloric acid with ultra-pure water. All measurements were performed for three times to obtain a satisfactory reproducibility.

Inhibitors diagnosis and measurements

The melting points of compounds were determined by Gallen Kamp (MFB-600) melting point apparatus. FT-IR spectra of compounds were recorded PERKIN ELMER SPEACTUM-65 within the range 4000–400 cm^{-1} using KBr Disk. The ^{1}H-NMR spectra were performed by Bruker 400 MHz spectrophotometer with TMS as internal standard, and deuterated DMSO was used as a solvent. The compounds were checked for their purity on silica gel TLC plates and the visualization of spots performed by using UV light.

Synthesis of inhibitors

General method for the synthesis of 4-amino-5-(substituted-phenyl)-4H [1, 2, 4] -triazole-3-thiols (ATT_1, ATT_2, ATT_4, ATT_5, ATT_6)

Figure 1 shows the scheme of synthesis procedure of inhibitors. The compounds were synthesized by the fusion of substituted benzoic acid (0.01 mol) and thiocarbohydrazide (0.015 mol), which contained in a round bottom flask and heated by a mantle until the content of the flask was melted [14, 15]. After cooling, the product was treated with sodium bicarbonate solution to neutralize the unreacted carboxylic acid, if any. It was then washed with water and collected by filtration. The completion of the reaction and the purity of the compound were checked by TLC (mobile phase hexane: ethyl acetate 1:2). The product was recrystallized from appropriate solvent to afford the title compounds.

Specifications of 4-(4-amino-5-mercapto-4H-1,2,4-triazole-3-yl) phenol (ATT_1)

White crystals, m.p: 216–218 °C, FT-IR (KBr, cm^{-1}): OH_{str} (3524(, NH_2 (3356), N–H_{str} (3144), aromatic C–H_{str} (3090), C=N_{str} (1654), aromatic C=C_{str} (1505, 1409), C=S (1244(, Yield: 60%. The spectrum of ^{1}H-NMR (400 MHz, d6-DMSO, ppm) to compound $\mathbf{ATT_1}$ appears to show the following data: δ H = 12.4 (S, 1 H, OH), 8.4 (S, 1 H, SH), 5.6–6.02 (4H, aromatic H), 5.2 (S, 2H, NH_2).

Specifications of 4-amino-5-(4-aminophenyl)-4H-1,2,4 -triazole-3-thiol (ATT_2)

Light gray crystals, m.p: 147–149 °C, FT-IR (KBr, cm^{-1}): NH_2 (3356, 3195), N–H_{str} (3137), aromatic C–H_{str} (2954), C=N_{str} (1647), aromatic C=C_{str} (1508, 1464), C=S (1248(, Yield: 63%.

Specifications of 4-amino-5-(4-((4-nitrobenzylidene)amino) phenyl)-4H-1,2,4-triazole-3-thiol (ATT_4)

Light yellow crystals, m.p: 208–210 °C, FT-IR (KBr, cm^{-1}): NH_2 (3381–3287), N–H_{str} (3141), aromatic C–H_{str} (2981), aliphatic C–H_{str} (2843), C=N_{str} (1607), aromatic C=C_{str} (1392), NO_2 (1341–1516), yield: 79%. The spectrum of ^{1}H-NMR (400 MHz, d6-DMSO, ppm) show the following data: δ H = 10.3 (S, 1 H, SH), 8.6 (S, 1H, N=CH), 8–8.2 (8H, aromatic H), 4.9 (S, 2H, NH_2). ^{13}C-NMR (400 MHz, d6-DMSO, ppm): δ C = 175 (CH=N), 140(N–C–N), 148, 147, 140, 135, 133, 129, 127, 123, 120 (Ar–CH).

Specifications of 4-amino-5-(4-((4-chlorobenzylidene) amino)phenyl)-4H-1,2,4-triazol-3-thiol (ATT_5)

Dark gray crystals, m.p:149–151 °C, FT-IR (KBr, cm^{-1}): NH_2(3422–3276), N–H_{str} (3115), aromatic C–H_{str} (2942), aliphatic C–H_{str} (2859), C=N_{str} (1610), C=C_{str} (1504), C–Cl_{str} (630), yield: 80%. The spectrum of ^{1}H-NMR 400 MHz, d6-DMSO, ppm to compound ATT_5 appears to show the following data: δ H = 8.7 (S, 1 H, SH), 8.2 (S, 2H, N=CH), 7.2–8 (4H, aromatic H), 5.4 (S, 2H, NH_2). ^{13}C-NMR (400 MHz, d6-DMSO, ppm): δ C = 163 (CH=N), 133(N–C–N), 141, 132, 129, 128, 127, 126, 123 (Ar–CH).

Specifications of 4-amino-5-(3,4-diaminophenyl)-4H-1,2,4 -triazole-3-thiole (ATT_6)

Deep brown crystals, m.p: < 300 °C, FT-IR (KBr, cm^{-1}): NH_2 (3363), N–H_{str} (3232), aromatic C–H_{str} (3151),

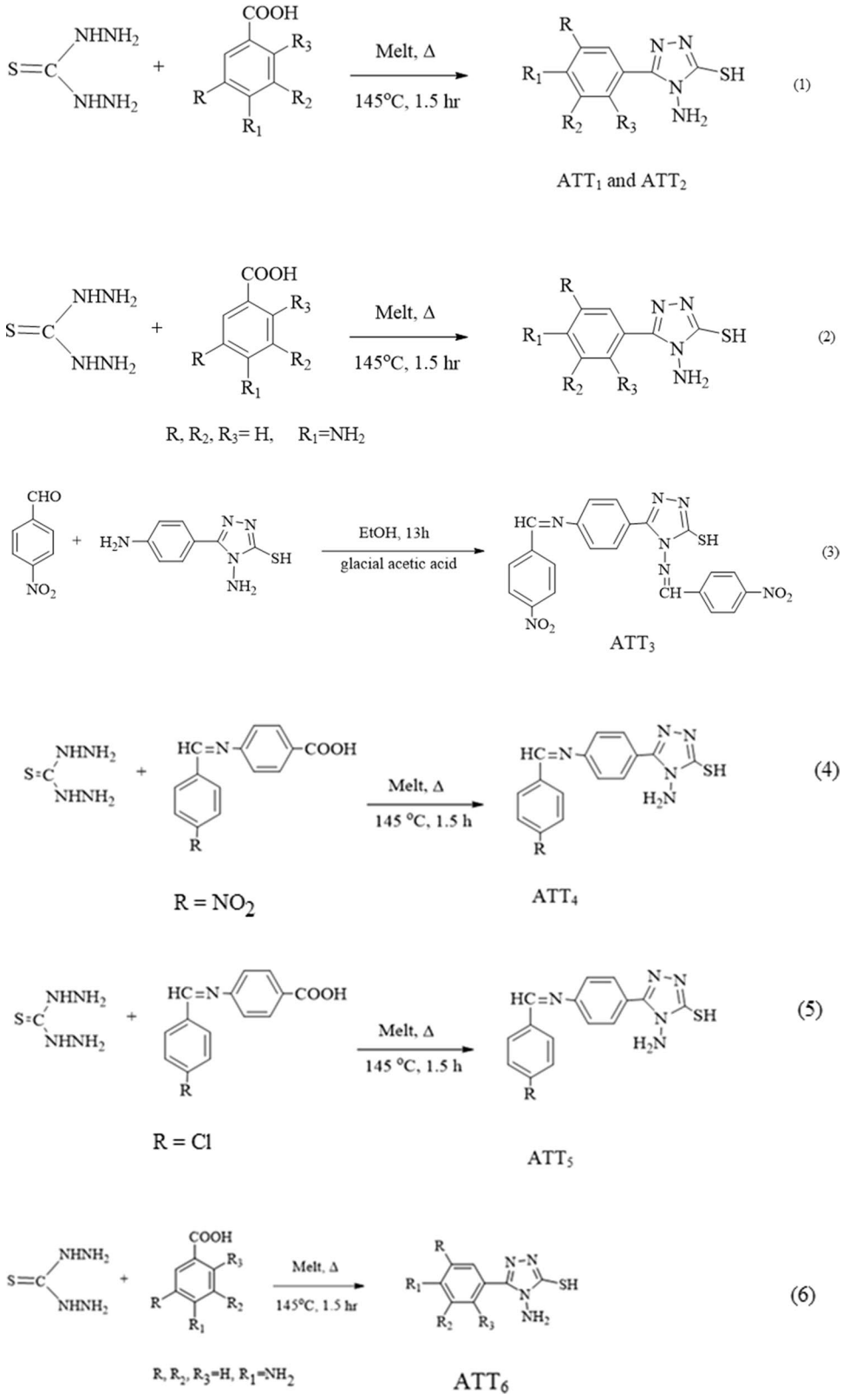

Fig. 1 Synthesis scheme of inhibitors

$C{=}N_{str}$ (1628), aromatic $C{=}C_{str}$ (1526, 1486), C=S (1274), yield: 80%.

General method for synthesis of 4-((4-nitrobenzylidene)amino)-5-(4- (((Z)-4-nitrobenzylidene)amino) phenyl)-4H-1,2,4-triazole-3-thiol (ATT_3)

A mixture of the compound ATT_2 (0.005 mol, 1.03 g) in 15 ml of absolute ethanol with a solution of 4-nitrobenzaldehyde (0.01 mol, 1.51 g) in 10 ml ethanol with five drops of glacial acetic acid as a catalyst and refluxed the mixture for 13 h [16]. The completion of the reaction and the purity of the compound were checked by TLC (mobile phase hexane: ethyl acetate 1:2) and then cooled the resultant solution to room temperature. The resulting yellow solid crystal 4-((4-nitrobenzylidene)amino)-5-(4-(((z)-4-nitrobenzylidene)amino)phenyl)-4H-1,2,4-triazole-3-thiol was filtered washed and recrystallized from appropriate solvent. The specifications of ATT3 were yellow crystals, m.p:233–235 °C, FT-IR (KBr, cm^{-1}):NH_2 (3297), $N{-}H_{str}$ (3122), aromatic $C{-}H_{str}$ (2990), $C{=}N_{str}$ (1599), $C{=}C_{str}$ (1442), $NO_{2\ str}$ (1343–1515), yield: 79%. The spectrum of ^{1}H-NMR (400 MHz, d6-DMSO, ppm) of ATT_3 appears to show the following data: δ H = 11.9 (S, 1 H, SH), 8.6 (S, 2H, N=CH), 7.6–8.2 (12H, aromatic H). ^{13}C-NMR (400 MHz, d6-DMSO, ppm): δC = 175 (CH=N), 130(N–C–N), 147, 128, 123, 112 (Ar–CH). Figures 2, 3, 4 and 5 show selected FT-IR and NMR curves of some

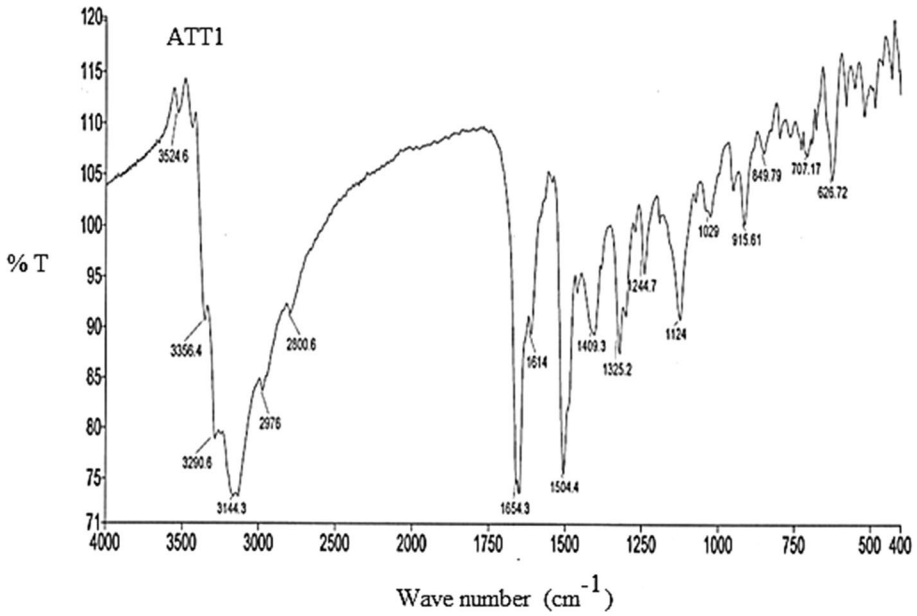

Fig. 2 FT-IR curve of ATT_1

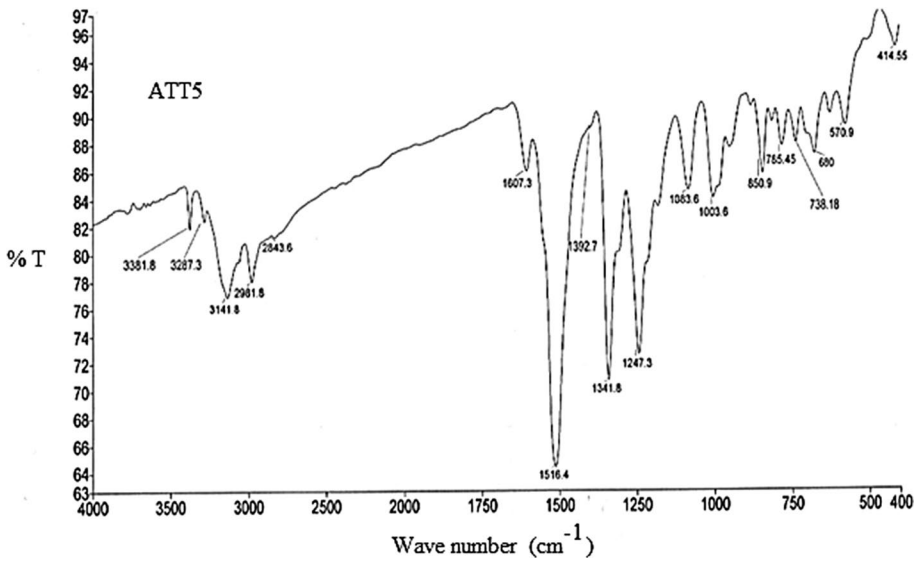

Fig. 3 FT-IR curve of ATT_5

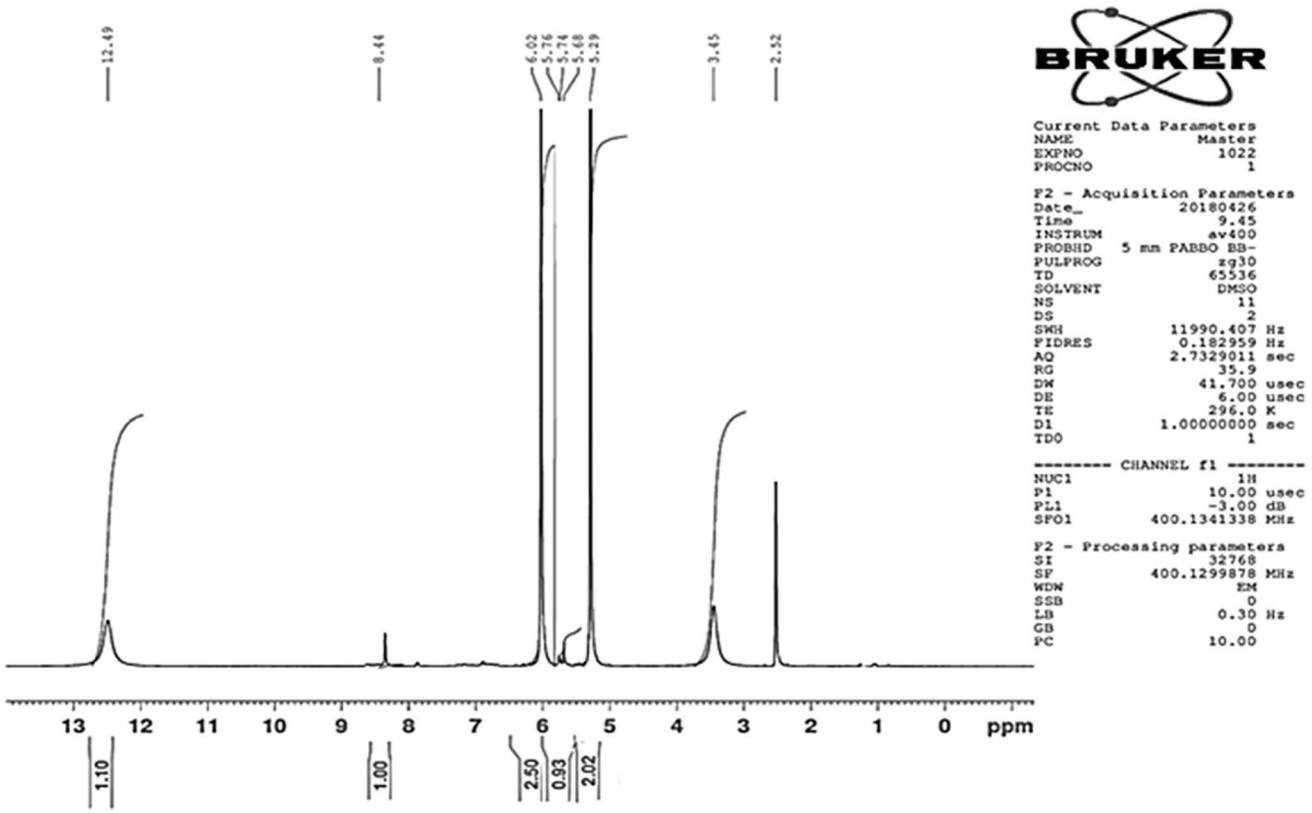

Fig. 4 ^{1}H-NMR spectra of compound ATT_1

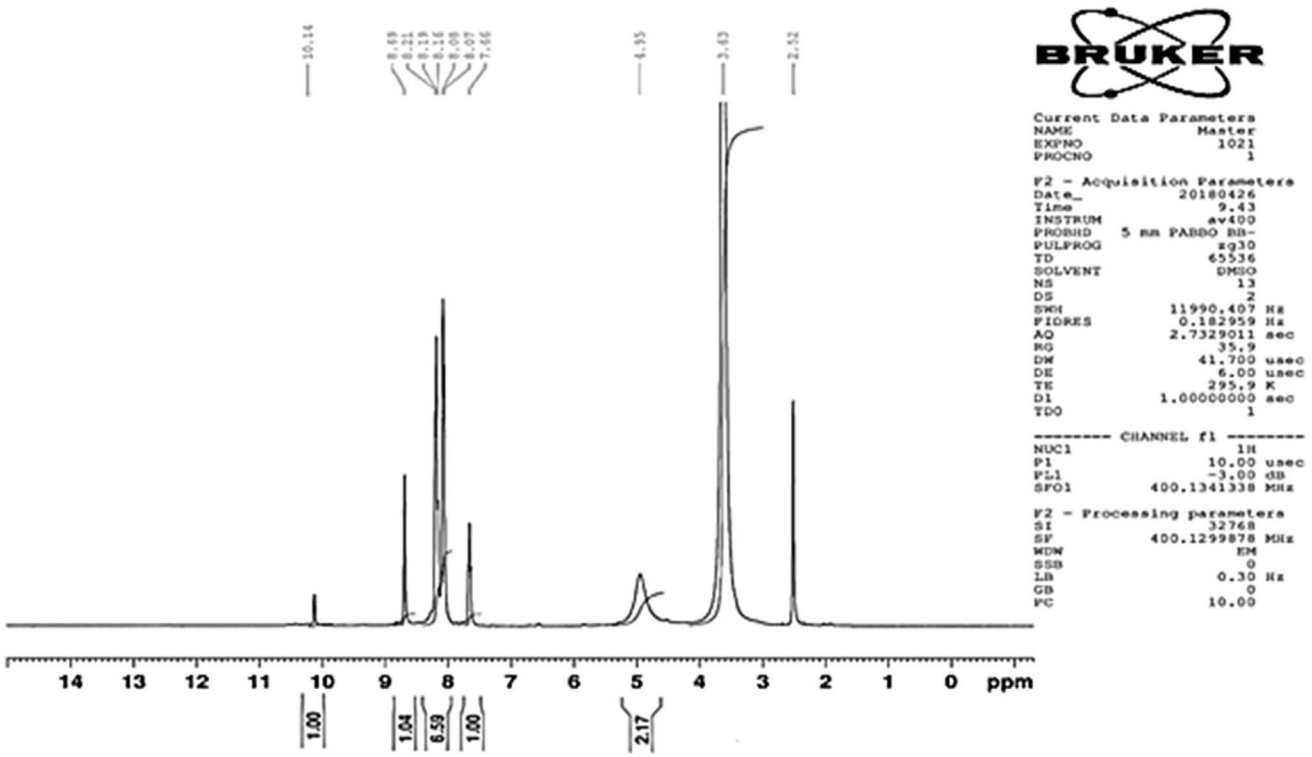

Fig. 5 ^{1}H-NMR spectra of compound ATT_4

Table 1 Physical property of the syntheses compounds

Compound	R	R_1	R_2	R_3	m.p. (°C)	Color	Molecular formula	Res. solvent	% Yield
ATT_1	H	OH	H	H	216–218	White	$C_8H_8N_4OS$	Ethanol/water	60
ATT_2	H	NH_2	NH_2	H	>300	Deep brown	$C_8H_{10}N_6S$	Ethanol/water	81
ATT_3	–	–	–	–	233–235	Yellow	$C_{22}H_{15}N_7O_4S$	Ethanol/water	79
ATT_4	NO_2	–	–	–	208–210	Light yellow	$C_{15}H_{12}N_6O_2S$	Ethanol/water	79
ATT_5	Cl	–	–	–	149–151	Dark gray	$C_{15}H_{12}N_5SCl$	Ethanol/water	80
ATT_6	H	NH_2	H	H	147–149	Light gray	$C_8H_9N_5S$	Ethanol/water	63

Table 2 Corrosion rate of low carbon steel alloy and inhibitor efficiency of synthesis compounds corrosion in 0.5 M hydrochloric acid solution at 30 °C and 0.001 M inhibitor concentration

Compounds	Formula	Corrosion rate (g m^2 day)	Inhibitor efficiency (%)
ATT_1	$C_8H_8N_4OS$	24.82	69.17
ATT_2	$C_8H_{10}N_6S$	25.79	67.97
ATT_3	$C_{22}H_{15}N_7O_4S$	28.17	65.02
ATT_4	$C_{15}H_{12}N_6O_2S$	39.92	50.43
ATT_5	$C_{15}H_{12}N_5SCl$	15.18	81.16
ATT_6	$C_8H_9N_5S$	31.86	60.43

synthesis inhibitors, while Table 1 collects the physical properties of compounds.

Weight loss measurements

Rectangular test specimens, with dimensions 3 cm × 1 cm × 0.1 cm, were made from low carbon steel, whose chemical composition as listed above. Samples were washed with running tap water followed by distilled water, dried with clean tissue, immersed in acetone and alcohol, dried again with clean tissue, then, kept in desiccators over silica gel bed until use. The dimensions of each sample were measured with a vernier to second decimal of millimeter and accurately weighted to the 4th decimal of gram. The metal samples were completely immersed each in 500 ml of uninhibited and inhibited 0.5 M HCl solution contained in a conical flask. They were exposed for a period of 3 h at the desired temperature and inhibitor concentration. Then, the metal samples were cleaned, washed with running tap water followed by distilled water dried with clean tissue then immersed in acetone and alcohol and dried again. Weight losses in gm m^{-2} day^{-1} (gmd) were determined in the presence and absence of inhibitor. At the beginning, all inhibitors were tested at inhibitor concentration of 0.001 M and 30 °C to select the best one. Then, the inhibitor with higher efficiency was evaluated at different temperature (30–60 °C) and inhibitor concentration of 1×10^{-3}, 2×10^{-3}, 3×10^{-3}, and 4×10^{-3} M.

Results and discussion

Weight loss measurements

Weight or mass loss technique is a very common and conventional method for corrosion rate evaluation. It was used in many researches as a powerful tool for metal loss estimation [17–19]. Table 2 summarizes the results of weight loss technique of the low carbon steel alloy corrosion in 0.5 M hydrochloric acid solution at 30 °C and 0.001 M inhibitor concentration. The values of corrosion rate were evaluated using the following equation [20]:

$$\mathrm{CR} = \frac{\text{weight loss } (g)}{\text{area } (\mathrm{m}^2) \times \text{time (day)}} \tag{7}$$

From the corrosion rate, the percentage inhibition efficiency of weight loss experiments (*IE*) was calculated using the following equation [21]:

$$\mathrm{IE} = \frac{\mathrm{CR}_{\text{uninibit}} - \mathrm{CR}_{\text{inhibit}}}{\mathrm{CR}_{\text{uninhibit}}} \times 100 \tag{8}$$

where $CR_{uninhibit}$ and $CR_{inhibit}$ are the corrosion rates in the absence and presence of inhibitors, respectively. Table 2 shows that inhibitor efficiency ranged from 50.43 to 81.16%. ATT_5 shows the higher performance. In order to have a clear vision of ATT_5 behavior, the effect of inhibitor concentration and temperature was studied. The results were shown in Table 3. Corrosion rate increased with increase in temperature and decrease in inhibitor concentration. While inhibitor efficiency increased with both increasing inhibitor concentration and temperature.

Effect of inhibitor concentration and adsorption isotherm

As shown in Table 3, at specific experimental temperature, corrosion rate of steel decreases with an increase in ATT_5 concentration. Values of inhibitor efficiency increase with increasing of ATT_5 concentration approach the maximum value of 95.8% at higher level of temperature and inhibitor

Table 3 Corrosion rate of low carbon steel alloy and inhibitor efficiency of synthesis ATT_5 corrosion in 0.5 M hydrochloric acid solution at different conditions

Test number	Inhibitor concentration (M)	Temperature (°C)	Corrosion rate (g/m^2. day)	Inhibitor efficiency (%)
1	0	20	33.99	–
2	0	30	80.52	–
3	0	40	142.96	–
4	0	50	419.21	–
5	1×10^{-3}	20	9.57	71.8
6	2×10^{-3}		8.36	75.4
7	3×10^{-3}		6.21	81.7
8	4×10^{-3}		5.06	85.1
9	1×10^{-3}	30	15.17	81.2
10	2×10^{-3}		15.05	81.3
11	3×10^{-3}		11.23	86.1
12	4×10^{-3}		10.75	86.6
16	1×10^{-3}	40	21.27	85.1
14	2×10^{-3}		18.47	87.1
15	3×10^{-3}		17.66	87.7
16	4×10^{-3}		16.83	88.3
17	1×10^{-3}	50	22.57	94.6
18	2×10^{-3}		20.52	95.1
19	3×10^{-3}		18.91	95.5
20	4×10^{-3}		17.66	95.8

concentration. This increase in inhibitor performance with temperature is apparently due to an increase in chemisorption of the inhibitor. Crucial step in the action of inhibitor behavior in acidic media is commonly agreed to be adsorption on the metal surface. This includes the assumption that the corrosion reactions are prevented from occurring over the area or active sites of the metal surface protected by adsorbed inhibitor molecules, whereas these corrosion reactions occurred generally on the inhibitor-free active sites [22]. The surface coverage (Θ = IE/100) data are very valuable in discussing the adsorption features. Surface covered is related to the concentration of inhibitor at constant temperature by well-known adsorption isotherm relationships that evaluated at equilibrium condition. The dependence of θ on the concentration of ATT_5 concentration was tested graphically by fitting it to Langmuir adsorption isotherm that assume a metal surface contains a fixed number of adsorption sites and each site took only one adsorbed molecule. Figure 6 shows linear plots for C/Θ versus C with average $R^2 = 0.999$ correlation coefficient, suggestion that the adsorption follows the Langmuir adsorption isotherm [23]:

$$\frac{C}{\theta} = \frac{1}{K} + C \tag{9}$$

where C is the inhibitor concentration, K adsorption equilibrium constant, representing the degree of adsorption, in other words the higher the value of K specifies that the ATT_5 molecules are strongly adsorbed on the metal surface. The slops of Langmuir adsorption lines are near unity meaning that each inhibitor molecules occupies one active site on the metal surface.

The standard adsorption free energy (ΔG_{ads}) was calculated using the following equation [23]:

$$K = \frac{1}{55.5}\exp\left(-\frac{\Delta G_{ads}}{RT}\right) \tag{10}$$

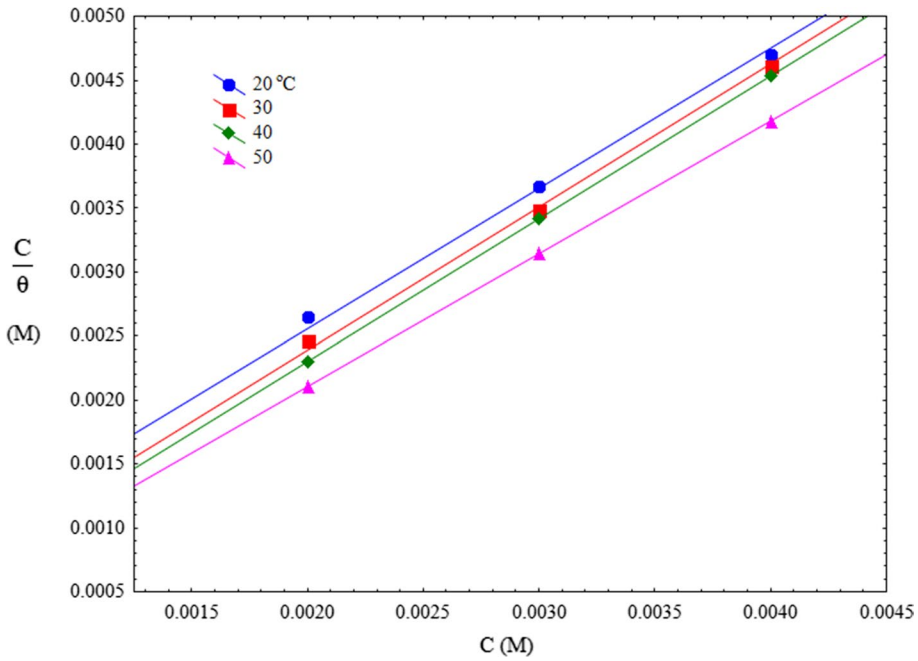

Fig. 6 Langmuir adsorption isotherms of ATT_5 on the steel surface in 0.5 M HCl solution at different temperatures

Table 4 Adsorption parameters of ATT_5 at different temperatures

T (°C)	K (M^{-1})	Slop	R^2	ΔG_{ads} (kJ mol^{-1})	ΔH_{ads} (kJ mol^{-1})	ΔS_{ads} (kJ mol^{-1} K^{-1})
20	2.5×10^3	1.09	0.99	−28.84	79.1	0.37
30	5×10^3	1.1	0.99	−31.57		
40	17.2×10^3	1.1	1.00	−35.84		
50	47.6×10^3	1.04	1.00	−39.71		
Average value	18.1×10^3	1.08	0.99	−33.99		

where 55.5 are the concentration of water in solution expressed in molar, R is gas constant, and T absolute temperature. Table 4 shows the adsorption parameters. The average value of standard adsorption free energy was −33.9 kJ mol^{-1}. The negative value of ΔG°_{ads} ensures the spontaneous adsorption process and stability of the adsorbed layer on the metal surface. Commonly, value of ΔG°_{ads} up to −20 kJ mol^{-1} is consistent with electrostatic interaction between the charged molecules and the charged metal (physical adsorption) while those around −40 kJ mol^{-1} or higher are associated with chemical adsorption as a result of sharing or transfer of electrons from the molecules to the metal surface to form a coordinate type of bond [24]. While other researchers suggested that the range of standard adsorption free energy of chemical adsorption processes for inhibitor in aqueous media lies between –21 and –42 kJ mol^{-1} [25]. Therefore, for present work, the values of adsorption heat have been considered within the range of chemical adsorption. It was also observed from Table 4, limited increase in the absolute value of ΔG_{ads} with an increase in temperatures, indicating that the adsorption was somewhat favorable with increasing experimental temperature and ATT_5 adsorbed according to chemical mechanism. The value of ΔH_{ads} was obtained from Van't Hoff equation (Eq. 11) [26] that drawn in Fig. 7. This figure shows good linear fitting.

The values of adsorption thermodynamic parameters for inhibitor can offer valuable information about the mechanism of corrosion inhibition. The endothermic adsorption process ($\Delta H_{ads} > 0$) is ascribed unequivocally to chemisorption, while generally, an exothermic adsorption process ($\Delta H_{ads} < 0$) may involve either physisorption or chemisorption or a mixture of both processes. In the present work; the positive sign of heat of adsorption (ΔH_{ads}) indicates that the adsorption of inhibitor is an endothermic process and the adsorption is chemisorption. This result agrees with above discussion.

While entropy of adsorption value (ΔS_{ads}) was obtained from Eq. 12 at average value of ΔG_{ads} and average temperature.

$$\ln K = -\frac{\Delta H_{ads}}{RT} + \text{constant} \tag{11}$$

$$\Delta S_{ads} = \frac{\Delta H_{ads} - \Delta G_{ads}}{T} \tag{12}$$

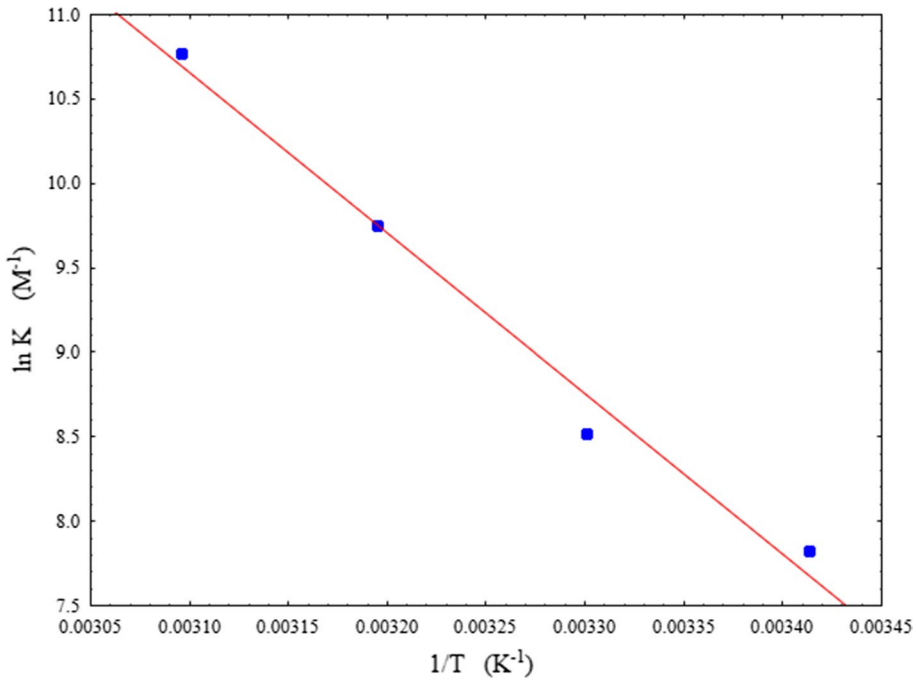

Fig. 7 Van't Hoff equation of ATT_5 on the steel surface in 0.5 M HCl solution at different temperatures

These results, which showed in Table 4, appear to contrast to that normally accepted for adsorption phenomena. It is well known that adsorption is an exothermic with a negative sign of adsorption heat accompanied by reduction entropy of adsorption [27]. In aqueous solution, the adsorption of organic molecules commonly is accompanied by desorption of water molecules. The adsorption of organic molecules at the metal–solution interface is a substitution adsorption process [28]. This means that each adsorbed molecule of ATT_5 on metal surface displaces water molecules from the surface. The thermodynamic values of ΔS_{ads} are the algebraic sum of the adsorption of ATT_5 molecules and the desorption of water molecules. Therefore, the increase in entropy is attributed to the increase in solvent entropy [29, 30]. Chaitra et al. [31] studied the effect of newly synthesized thiazole hydrazones on the corrosion of mild steel in 0.5 M hydrochloric acid. Adsorption of the inhibitors followed Langmuir isotherm and addition of inhibitors simultaneously decreased corrosion rate.

Tezcan et al. [32] investigated newly synthesized sulfur containing Schiff base (4-((thiophene-2-ylmethylene)amino) benzamide) compound. Inhibition performance on mild steel in 1.0 M HCl solution was studied. The results showed that the highest inhibitor efficiency of 96.8%.

Messali et al. [33] studied the inhibition effect and adsorption behavior of 4-((2,3-dichlorobenzylidene)amino)-3-methyl-1H-,2,4-triazole-5(4H)-thione on mild steel in 1 M HCl solution. The inhibitor can be adsorbed onto surface by both physical and chemical means obeys Langmuir adsorption isotherm.

Effect of temperature and activation parameters

As shown in Table 5, at specific experimental temperature, corrosion rate of steel decreases with an increase in ATT_5 concentration. The kinetics of the ATT_5 action can be realized by comparing the activation parameters in the presence and absence of the inhibitor. Activation energy (E_a), enthalpy of activation (ΔH_a), and entropy of activation (ΔS_a) for both uninhibited and inhibited 0.5 M hydrochloric acid steel corrosion at different temperatures and acid concentration were evaluated from an Arrhenius-type plot (Eq. 13) and transition state theory (Eq. 14) [34]:

$$\mathrm{CR} = A \ \exp\left(-\frac{E_a}{\mathrm{RT}}\right) \tag{13}$$

$$\mathrm{CR} = \frac{\mathrm{RT}}{Nh} \ \exp\left(\frac{\Delta S_a}{R}\right) \exp\left(-\frac{\Delta H_a}{\mathrm{RT}}\right) \tag{14}$$

where CR is the corrosion rate, A is the Arrhenius constant, R is the universal gas constant, h is Plank's constant, and N is Avogadro's number. As shown in Fig. 8, plot of ln (CR) versus $1/T$ gives straight lines with slopes of $\Delta E_a/R$ and intercept can be used for evaluating of A. While, Fig. 9 shows a liner straight lines of ln (CR/T) versus $1/T$ slopes of $\Delta H_a/R$ and intercept can be used for evaluating of ΔS_a. Table 5 illustrates the activation parameters for steel corrosion reaction acidic solution at different conditions. It is clearly shown that the activation energy and enthalpy vary in similar way. The activation energy and activation enthalpy for uninhibited acid were higher than inhibited one. The decrease in the value of activation energy and enthalpy appears to be unreliable. However, this may be attributed to increase in metal surface coverage by the inhibitor molecules at higher temperatures and also suggested that the formation rate of the chemisorbed layer may be greater than its rate of dissolution at higher temperatures [35]. Other researchers [36] found that some anticorrosion materials in the acidic solutions alter the kinetics of corrosion reaction by proposing alternate reaction paths with lower activation energies. Table 4, illustrates also that all the values of frequency factor are lower than uninhibited one, which is benefit for inhibiting the corrosion rate of steel. It is also well known that the increase in A raises the corrosion rate of steel [37]. Furthermore, at all cases, the values of E_a are higher than ΔH_a by a value which approximately equal to RT, which confirm the thermodynamic principle of the reactions are characterized by following equation [38]:

$$E_a - \Delta H_a = \mathrm{RT} \tag{15}$$

The negative value of ΔS_a for both cases of absence and presence of inhibitor indicates that activated complex in the rate determining step denotes an association rather than a dissociation step, which means a decrease in disorder, takes place during the course of transition from reactant to the activated complex [39].

Khan et al. [40] studied the inhibitory effect of two Schiff bases 3-(5-methoxy-2-hydroxybenzylideneamino)-2-(-5-methoxy-2-hydroxyphenyl)-2,3-dihydroquinazoline-4(1H)-one (MMDQ), and 3-(5-nitro-2-hydroxybenzylideneamino)-2(5-nitro-2-hydroxyphenyl)-2,3-dihydroquinazoline-4(1H)-one (NNDQ) on the corrosion of mild steel in 1 M

Table 5 Activation parameters for steel corrosion reaction in uninhibited and inhibited 0.5 M HCl

C (M)	A (gmd)	E_a (kJ mol^{-1})	ΔH_a (kJ mol^{-1})	ΔS_a (J mol^{-1} K^{-1})
0	7.3×10^{12}	63.67	61.12	− 7.98
1×10^{-3}	1.3×10^{5}	23.09	20.54	− 155.22
2×10^{-3}	1.2×10^{5}	23.04	20.48	− 156.21
3×10^{-3}	1.6×10^{6}	30.09	27.54	− 134.74
4×10^{-3}	5.2×10^{6}	33.36	30.81	− 124.87

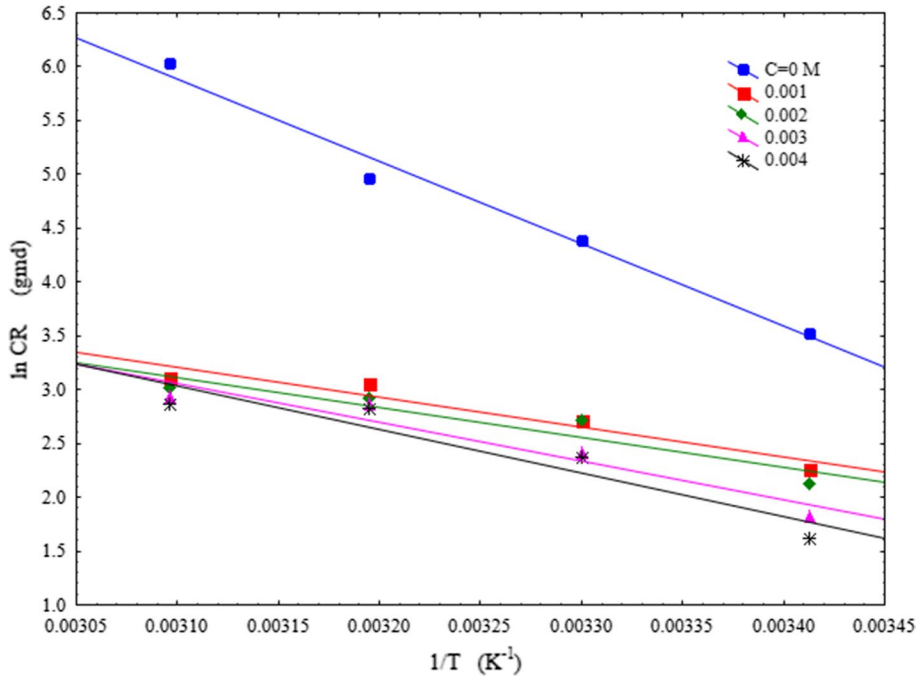

Fig. 8 Arrhenius plots of steel in uninhibited and inhibited 0.5 M HCl

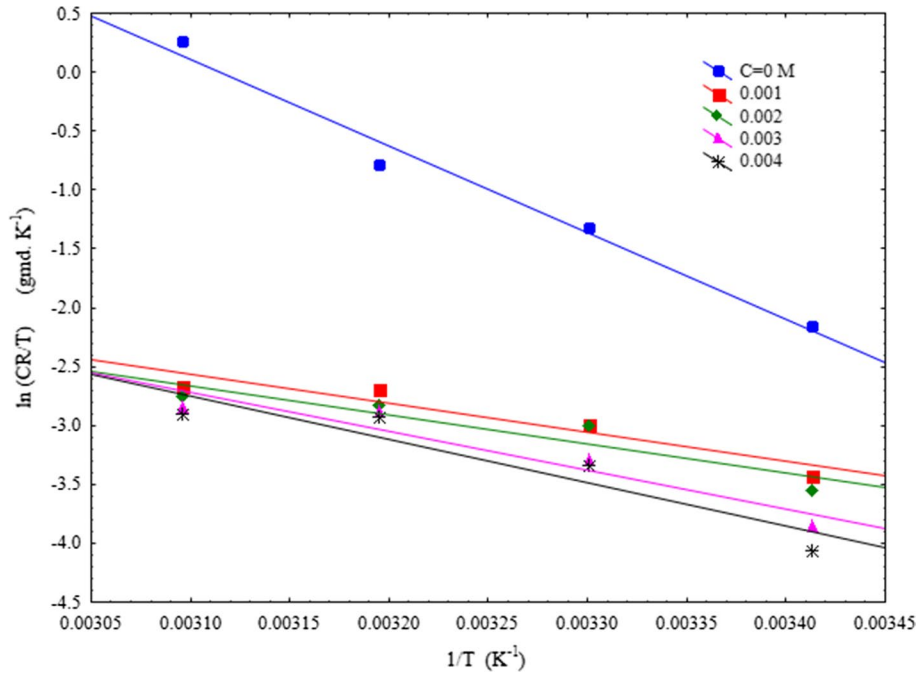

Fig. 9 Transition—state plots of steel in uninhibited and inhibited 0.5 M HCl

hydrochloric acid. The effect of temperature on the inhibition process in 1 M HCl with the addition of inhibitors was investigated at a temperature range of 30–60 °C. Corrosion rate increased with raise in temperature, and the efficiencies of the investigated inhibitors are strongly temperature dependent. Enthalpy, entropy and enthalpy of activation were calculated. The result showed that *Enthalpy of activation* for solution containing inhibitors are lower than those in the inhibitor-free acid solution can be attributed to its chemisorption on mild steel surface. Similar results were obtained by Obaid et al. [41]. The lower values of *activation energy* in the presence of the inhibitors and the general increase in their inhibitor efficiencies with increasing temperatures are indicative of chemisorption (interaction of unshared electron pairs in the adsorbed molecule with the metal) of these compounds on the steel surface.

Quantum chemical and theoretical calculations

Quantum chemical calculations have been widely used to investigate reaction mechanism of inhibition process [42]. It is also verified to be a very important tool for studying corrosion control mechanism and to obtain insight view to the inhibition mechanism of ATT_5 inhibitor. By using of quantum chemical calculations, the structural parameters, such as HOMO (highest occupied molecular orbital), LUMO (lowest unoccupied molecular orbital), dipole moment (μ) and fraction of electron transferred (ΔN), were calculated. The structures of inhibitors were optimized by *ChemoOffice* version 14 software. Figure 10 shows the optimized structures, HOMO and the LUMO structure of all synthesis inhibitors. The calculated quantum chemical properties are summarized in Table 6. As shown in Fig. 10, both the HOMO and LUMO distributions of synthesis inhibitors were concentrated mainly over sulfur and nitrogen atoms. E_{LUMO} and E_{HOMO} characterized the electron-receiving and—donating capability of synthesis inhibitors. In general, a low E_{LUMO} implies that inhibitors tend to accept electrons, while a high E_{HOMO} refer to a strong electron donating [43]. Energy gap (ΔE) specifies the chemical stability of inhibitors, and a lower energy gap value typically leads to higher adsorption on the metal surface, resulting in greater inhibition efficiencies [44]. The order of inhibition efficiency was $ATT_5 > ATT_1 > ATT_2 > ATT_3 > ATT_6 > ATT_4$, while the order of energy gap was $ATT_5 > ATT_4 > ATT_3 > ATT_2 > ATT_6 > ATT_1$. The differences in orders may be attributed to close inhibition efficiencies of inhibitors. As seen in Table 2, the value of inhibitor efficiencies were 60.43, 65.02, 67.97, and 69.17% for ATT_6, ATT_3, ATT_2 and ATT_1, respectively, which is very close range. However, still ATT_5 has the lower energy gap that confirms the experimental work. The number of transferred electrons (ΔN) was also calculated according to Eq. 16 [45].

$$\Delta N = \frac{X_{Fe} - X_{inh}}{2(\eta_{Fe} + \eta_{inh})} \tag{16}$$

where X_{Fe} and X_{inh} denote the absolute electronegativity of iron and the MLH inhibitor molecule, respectively; η_{Fe} and η_{inh} denote the absolute hardness of iron and the inhibitor molecule, respectively. These quantities are related to electron affinity (A) and ionization potential (I) that both related in turn to E_{HOMO} and E_{LUMO}:

$$\begin{aligned} X &= \frac{I + A}{2} = \frac{-(E_{HOMO} + E_{LUMO})}{2} \\ \eta &= \frac{I - A}{2} = \frac{-(E_{HOMO} - E_{LUMO})}{2} \end{aligned} \tag{17}$$

Values of X and η were considered by using the values of I and A gained from quantum chemical calculation. The theoretical value of X_{Fe} is 7 according to Pearsons electronegativity scale and η_{Fe} is 0 eV/mol, respectively [46]. The fraction of electrons transferred from inhibitor to the steel surface (ΔN) was calculated and listed in Table 3. According to Lukovits [47], if $\Delta N < 3.6$, the inhibition efficiency increased with increasing electron-donating ability at the steel surface. In this study, synthesis inhibitors were the donor of electrons, and the metal surface was the acceptor. This result supports the assertion that the adsorption of inhibitors on the steel surface can occur on the bases of donor–acceptor interactions between the ℼ electrons of the compound and the vacant d-orbitals of the metal surface. The dipole moment (μ) is also a significant factor and there is lack of agreement on the relation between μ and inhibitive performance. Some researchers founded that a low μ value will favor accumulation of the inhibitor on metal surface and increasing the inhibitor performance [48, 49]. While others researches suggested that a high value of dipole moment associated with the dipole–dipole interaction of inhibitor and metal surface can enhance the adsorption on the metal surface and increasing efficiency [50, 51]. In present work, the value of μ for ATT_5 was the lowest one among all tested inhibitors that agree with the first opinion. The anodic oxidation behavior of steel in HCl acid can be explained by following reaction [52]:

$$Fe + Cl^- \leftrightarrow (FeCl^-)_{ads} \tag{18}$$

$$(FeCl^-)_{ads} \leftrightarrow (FeCl)_{ads} + e^- \tag{19}$$

$$(FeCl)_{ads} \rightarrow \left(FeCl^+\right)_{ads} + e^- \tag{20}$$

$$\left(FeCl^+\right)_{ads} \rightarrow Fe^{2+} + Cl^- \tag{21}$$

While the cathodic hydrogen evolution reaction can be written as:

$$Fe + H^+ \leftrightarrow \left(FeH^+\right)_{ads} \tag{22}$$

$$\left(FeH^+\right)_{ads} + e^- \rightarrow (FeH)_{ads} \tag{23}$$

$$(FeH)_{ads} + H^+ + e^- \rightarrow Fe + H_2 \tag{24}$$

According to the structures of the synthesis inhibitors, there are the free electron pairs on N and S that able to forming **σ-bond with iron [53]. In addition, in case of acidic solution, electrostatic interaction is possible between the negatively charge of iron surface that may be brought about by specific adsorption of Cl^- anions and the positively charged inhibitor. The essential effect of inhibitors is due to the presence of free electron pairs in the N and S atoms, p-electrons on the aromatic ring, type of interaction with the steel surface, and metallic complexes formation. It

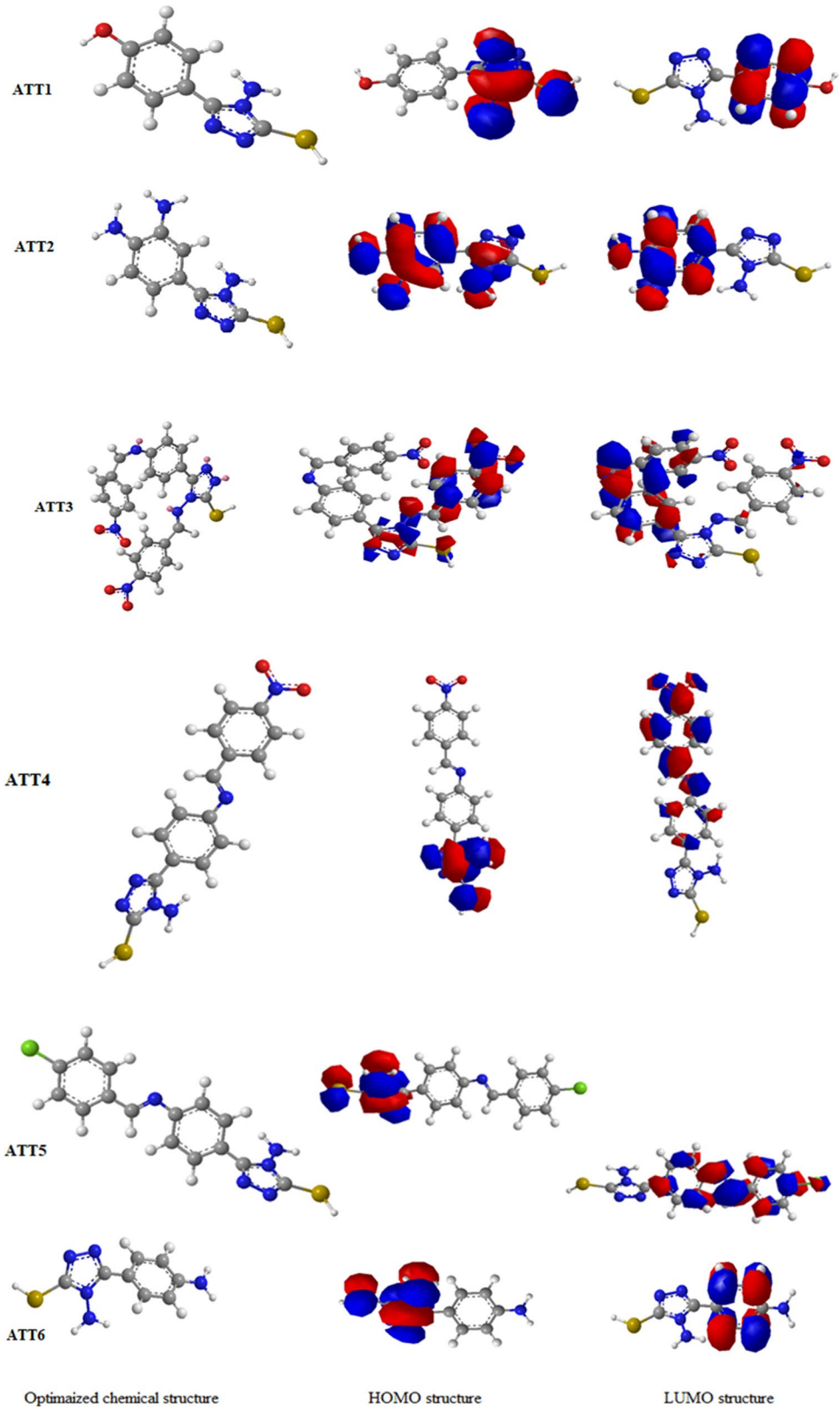

Fig. 10 Optimized chemical structures of six inhibitors and HOMO–LUMO distribution

is well known that steel has coordination affinity toward N and S bearing ligand. Therefore, adsorption on metal surface can be ascribed to coordination through heteroatoms and p-electrons of aromatic rings [54]. In the present case, synthesis inhibitors, there are unshared electron pairs on N and S, able to form σ-bond with steel.

Table 6 Quantum chemical parameters for inhibitors

Compounds	E_{HOMO} (eV)	E_{LUMO} (eV)	ΔE (eV)	ΔN	Dipole (debye)
ATT_1	−7.654	−1.068	6.586	−0.401	4.685
ATT_2	−7.186	−2.160	5.026	−0.462	5.691
ATT_3	−7.511	−2.613	4.898	−1.013	5.855
ATT_4	−7.683	−4.574	3.109	0.115	6.942
ATT_5	−7.654	−5.322	2.332	−0.303	4.362
ATT_6	−7.605	−1.068	6.537	0.407	6.124

Conclusion

The following points can be concluded from present work:

1. The six inhibitors were synthesis and test successfully as corrosion inhibitors for steel in acidic solution.
2. Experimental results show that the order of inhibition efficiency was $ATT_5 > ATT_1 > ATT_2 > ATT_3 > ATT_6 > ATT_4$.
3. The addition of ATT_5 to the 0.5 M HCl solution at different temperature and inhibitor concentration reduces corrosion of mild steel with inhibitor efficiency exceed 95%.
4. Inhibitor efficiency of ATT_5 increased with an increase in the inhibitor concentration. The high inhibition efficiency of inhibitor was attributed to the formation of a layer on the steel surface.
5. Adsorption follows Langmuir adsorption isotherm with high negative value of heat of adsorption, which indicates the formation of chemical layer on metal surface.

Acknowledgements The authors would like to thank Department of Chemistry—College of Science—University of Diyala for continuous support and facilities.

References

1. Verma C, Olasunkanmi LO, Obot IB, Ebenso EE, Quraishi MA (2016) 2, 4-Diamino-5- (phenylthio)-5 H-chromeno [2, 3-b] pyridine-3-carbonitriles as green and effective corrosion inhibitors: gravimetric, electrochemical, surface morphology and theoretical studies. RSC Adv 6:53933–53948
2. Sasikumar Y, Adekunle AS, Olasunkanmi LO, Bahadur Baskar IR, Kabanda MM, Obot IB, Ebenso EE (2015) Experimental, quantum chemical and Monte Carlo simulation studies on the 15 corrosion inhibition of some alkyl imidazolium ionic liquids containing tetrafluoroborate anion on MSin acidic medium. J Mol Liq 211:105–118
3. Khadiri R, Bekkouche K, Aouniti A, Hammouti B, Benchat N, Bouachrine M, Solmaz R (2016) Gravimetric, electrochemical and quantum chemical studies of some pyridazine derivatives as corrosion inhibitors for mild steel in 1 M HCl solution. J Taiwan Inst Chem Engg 58:552–564
4. Khadom A, Yaro A, Altaie A, Kaduim A (2009) Electrochemical, activations and adsorption studies for the corrosion of low carbon steel in acidic media. Port Electrochem Acta 27(2009):699–712
5. Musa A, Kaduim A, Abu Bakar M, Takriff M, Daud Abdul Razak, Kamarudin Siti Kartom (2010) On the inhibition of mild steel corrosion by 4-amino-5-phenyl-4H-1, 2,4-trizole-3-thiol. Corros Sci 52:526–533
6. Khadom A, Musa A, Kaduim A, Abu Bakar M, Takriff M (2010) Adsorption kinetics of 4-Amino-5-Phenyl-4H-1, 2, 4-Triazole-3-thiol on mild steel surface inhibitor. Port Electrochim Acta 28:221–230
7. Alaneme K, Daramola Y, Olusegun S, Afolabi A (2015) Corrosion inhibition and adsorption characteristics of rice husk extracts on mild steel immersed in 1 M H_2SO_4 and HCl solutions. Int J Electrochem Sci 10:3553–3567
8. Noor E, Al-Moubaraki A (2008) Thermodynamic study of metal corrosion and inhibitor adsorption processes in mild steel/1-methyl-4[4 (-X)-styryl pyridinium iodides/hydrochloric acid systems. Mater Chem Phys 110:145–154
9. Bentiss F, Lebrini M, Lagrenee M (2005) Thermodynamic characterization of metal dissolution and inhibitor adsorption processes in mild steel/2,5-bis(n-thienyl)-1,3,4-thiadiazoles/hydrochloric acid system. Corros Sci 47:2915–2931
10. Popova A, Christov M, Zwetanova A (2007) Effect of the molecular structure on the inhibitor properties of azoles on mild steel corrosion in 1 M hydrochloric acid. Corros Sci 49:2131–2143
11. Bhrara K, Kim H, Singh G (2008) Inhibiting effects of butyl triphenyl phosphonium bromide on corrosion of mild steel in 0.5 M sulphuric acid solution and its adsorption characteristics. Corros Sci 50:2747–2754
12. Sudheer M, Quraishi A (2014) 2-Amino-3,5-dicarbonitrile-6-thio-pyridines: new and effective corrosion inhibitors for mild steel in 1 M HCl. Ind Eng Chem Res 53:2851–2859
13. Musa A, Kadhum A, Mohamad A, Takriff M (2010) Experimental and theoretical study on the inhibition performance of triazole compounds for mild steel corrosion. Corros Sci 52:3331–3340
14. Gupta A, Prachand S, Patel A, Jain S (2012) Synthesis of some 4-Amino-5-(substituted-phenyl)-4H-[1, 2, 4] triazole-3-thiol derivatives and antifungal activity. Int J Pharm Life Sci 3:1848–1857
15. Aly A, Brown A, El-Emary T, Ewas A, Ramadan M (2009) Hydrazinecarbothioamide group in the synthesis of heterocycles. Arkivoc I:150–197

16. Hadi Kadhim S, Qahtan Abd-Alla I, Jawad Hashim T (2017) Synthesis and characteristic study of Co(II), Ni(II) and Cu(II) complexes of new schiff base derived from 4-amino antipyrine. Int J Chem Sci 15:107–115
17. Khadom A, Abd A, Ahmed N (2018) Xanthium strumarium leaves extracts as a friendly corrosion inhibitor of low carbon steel in hydrochloric acid: kinetics and mathematical studies. S Afr J Chem Eng 25:13–21
18. Khadom A, Abd A, Ahmed N (2018) Potassium iodide as a corrosion inhibitor of mild steel in hydrochloric acid: kinetics and mathematical studies. J Bio Tribo Corros 4(17):2–10
19. Hassan K, Khadom A, Kurshed N (2016) Citrus aurantium leaves extracts as a sustainable corrosion inhibitor of mild steel in sulfuric acid. S Afr J Chem Eng 22:1–5
20. Khadom A (2015) Kinetics and synergistic effect of halide ion and naphthylamin for inhibition of corrosion reaction of mild steel in hydrochloric acid. React Kinet Mech Catal 115:463–481
21. Khadom AA, Abod BM, Mahood HB, Kadhum AAH (2018) Galvanic corrosion of steel–brass couple in petroleum waste water in presence of a green corrosion inhibitor: electrochemical, kinetics, and mathematical view. J Fail Anal Preven 18:1300–1310
22. Yaro A, Khadom A, Ibraheem H (2011) Peach juice as an anticorrosion inhibitor of mild steel. Anti-Corrosion Methods Mater 58(3):116–124
23. Khadom A, Yaro A, AlTaie A, Kadum A (2009) Electrochemical, activations and adsorption studies for the corrosion inhibition of low carbon steel in acidic media. Port Electrochim Acta 27:699–712
24. Noor E (2009) Evaluation of inhibitive action of some quaternary N-heterocyclic compounds on the corrosion of Al–Cu alloy in hydrochloric acid. Mater Chem Phys 114:533–541
25. Umoren S, Ebenso E (2007) The synergistic effect of polyacrylamide and iodide ions on the corrosion inhibition of mild steel in H_2SO_4. Mater Chem Phys 106:393
26. Obot I, Obi-Egbedi N (2010) An interesting and efficient green corrosion inhibitor for aluminium from extracts of Chlomolaena odorata L. in acidic solution. J Appl Electrochem 40:1977–1984
27. Amar H, Benzakour J, Derja A, Villemin D, Moreau B, Braisaz T (2006) Piperidin-1-yl-phosphonic acid and (4-phosphono-piperazin-1-yl) phosphonic acid: a new class of iron corrosion inhibitors in sodium chloride 3% media. Appl Surf Sci 252(6162):6166
28. Umoren S, Ebenso E (2007) The synergistic effect of polyacrylamide and iodide ions on the corrosion inhibition of mild steel in H_2SO_4. Mater Chem Phys 106:387–393
29. Li X, Deng SD, Fu H, Mu GN (2010) Synergistic inhibition effect of rare earth cerium(IV) ion and sodium oleate on the corrosion of cold rolled steel inphosphoric acid solution. Corros Sci 52:1167–1178
30. Fadhil Ahmed A, Khadom AA, Liu Hongfang, Chaoyang Fu, Wang Junlei, Fadhil Noor A, Mahood Hameed B (2019) (S) 6 Phenyl 2,3,5,6 tetrahydroimidazo[2,1 b] thiazole hydrochloride as corrosion inhibitor of steel in acidic solution: gravimetrical, electrochemical, surface morphology and theoretical simulation. J Mol Liq 276:503–518
31. Chaitra TK, Mohana KN, Gurudatt DM, Tandon HC (2016) Inhibition activity of new thiazole hydrazones towards mild steel corrosion in acid media by thermodynamic, electrochemical and quantum chemical methods. J Taiwan Inst Chem Eng 67:521–531
32. Tezcan F, Yerlikaya G, Mahmood A, Kardaş G (2018) A novel thiophene Schiff base as an efficient corrosion inhibitor for mild steel in 1.0 M HCl: electrochemical and quantum chemical studies. J Mol Liq 269:398–406
33. Messali M, Larouj M, Lgaz H, Rezki N, Al-Blewi FF, Aouad MR, Chaouiki A, Salghi R, Chung I (2018) A new Schiff base derivative as an effective corrosion inhibitor for mild steel in acidic media: experimental and computer simulations studies. J Mol Struct 1168:39–48
34. Musa A, Kadhum A, Mohamad A, Takriff M, Daud A, Kamarudin S (2010) On the inhibition of mild steel corrosion by 4-amino-5-phenyl-4H-1, 2, 4-trizole-3-thiol. Corros Sci 52:526–533
35. Ahmed SK, Ali WB, Khadom AA (2019) Synthesis and characterization of new triazole derivativesas corrosion inhibitors of carbon steel in acidic medium. J Bio Tribo-Corros 5:15
36. Khadom AA, Yaro AS (2011) Protection of low carbon steel in phosphoric acid by potassium iodide. Prot Metals Phys Chem Surf 47:662–669
37. Benabdellah M, Touzani R, Dafali A, Hammouti B, El Kadiri S (2007) Ruthenium–ligand complex, an efficient inhibitor of steel corrosion in H_3PO_4 media. Mater Lett 61:1197–1204
38. Noor EA, Al-Moubaraki AH (2008) Thermodynamic study of metal corrosion and inhibitor adsorption processes in mild steel/1 methyl-4[4′(-X)-styryl pyridinium iodides/hydrochloric acid systems. Mater Chem Phys 110:145–154
39. Ramesh Saliyan V, Adhikari V, Airody A (2007) Inhibition of corrosion of mild steel in acid media by N0-benzylidene-3-(quinolin-4-ylthio)propanohydrazide. Bull Mater Sci 31:699–711
40. Khan G, Basirun WJ, Kazi SN, Ahmed P, Magaji L, Ahmed SM, Khan GM, Rehman MA, Mohamad Badry AB (2017) Electrochemical investigation on the corrosion inhibition of mild steel by Quinazoline Schiff base compounds in hydrochloric acid solution. J Colloid Interface Sci 502:134–145
41. Obaid AY, Ganash AA, Qusti Shabaan AH, Elroby A, Hermas AA (2017) Corrosion inhibition of type 430 stainless steel in an acidic solution using a synthesized tetra-pyridinium ring-containing compound. Arab J Chem 10(Supplement 1):S1276–S1283
42. Guo L, Zhu S, Zhang S, He Q, Li W (2014) Theoretical studies of three triazolederivatives as corrosion inhibitors for mild steel in acidic medium. Corros Sci 87:366–375
43. Zhang D, Tang Y, Qi S, Dong D, Cang H, Lu G (2016) The inhibition performance of long-chain alkyl-substituted benzimidazole derivatives for corrosion of mild steel in HCl. Corros Sci 102:517–522
44. Hu K, Zhuang J, Ding J, Ma Z, Wang F, Zeng X (2017) Influence of biomacromolecule DNA corrosion inhibitor on carbon steel. Corros Sci 125:68–76
45. Mourya P, Singh P, Tewari A, Rastogi R, Singh M (2015) Relationship between structure and inhibition behavior of quinolinium salts for mild steel corrosion: experimental and theoretical approach. Corros Sci 95:71–87
46. Pearson RG (1988) Absolute electronegativity and hardness: application to inorganic chemistry. Inorg Chem 27:734–740
47. Lukovits I, Lalman E, Zucchi F (2001) Corrosion inhibitors—correlation between electronic structure and efficiency. Corrosion 57:3–8
48. Qiang Y, Guo L, Zhang S, Li W, Yu S, Tan J (2016) Synergistic effect of tartaric acid with 2,6-diaminopyridine on the corrosion inhibition of mild steel in 0.5 M HCl. Sci Rep 6: 33305
49. Li LJ, Zhang XP, Lei JL, He JX, Zhang ST, Pan FS (2012) Adsorption and corrosion inhibition of Osmanthus fragran leaves extract on carbon steel. Corros Sci 63:82–90
50. Yüce A, Do˘grumert B, Kardas G, Yazıcı B (2014) Electrochemical andquantum chemical studies of 2-amino-4-methyl-thiazole as corrosioninhibitor for mild steel in HCl solution. Corros Sci 83:310–316
51. Zheng X, Zhang S, Li W, Gong M, Yin L (2015) Experimental and theoretical studiesof two imidazolium-based ionic liquids as inhibitors for mild steel in sulfuricacid solution. Corros Sci 95:168–179
52. Kumari P, Shetty P, Rao S (2017) Electrochemical measurements for the corrosion inhibition of mild steel in 1 M hydrochloric acid by using an aromatic hydrazide derivative. Arab J Chem 10:653–663
53. Rashid K, Khadom A (2018) Adsorption and kinetics behavior of kiwi juice as a friendly corrosion inhibitor of steel in acidic media. World J Eng 15(3):388–401

54. Ahmad I, Prasad R, Quraishi M (2010) Inhibition of mild steel corrosion in acid solution by pheniramine drug: experimental and theoretical study. Corros Sci 52:3033–3341